The Effect of Bilayer Periods and Their Thickness in Magnetron Sputtering Protective Multilayer Coatings for Tribological Applications

Khalil Aouadi, Corinne Nouveau, Aurélien Besnard, Brahim Tlili, Alex Montagne, and Moez Chafra

CrN/CrAlN thin films were deposited by DC reactive magnetron sputtering. The influence of CrN/CrAlN bilayer thickness on the microstructure, mechanical, and tribological properties was studied. Crystallinity of the layers was characterized by x-ray diffraction. The microstructure of all coatings was observed by scanning electron microscopy. Results exhibit that bilayer thickness was a dominant factor. The analyses showed a columnar microstructure for the CrN/CrAlN coatings. Owing to their denser structure and interfacial strengthening, CrN/CrAlN multilayer coatings exhibited higher mechanical properties than that of monolayers. Indeed, CrN/CrAlN multilayer coating with four bilayers and thickness gradient reaches a maximum of hardness around 43 GPa. Also, its resistance to spallation reaches 97 N which is a very excellent value. After ball-on-disk wear tests, it is found that all multilayer films exhibited a good wear resistance, especially the one with four bilayers and different CrN and CrAlN monolayers thickness. The lowest coefficient of friction is obtained for the coatings with 4 bilayers.

Keywords bilayer period, CrN/CrAlN, mechanical properties, microstructure, wear

1. Introduction

The physical vapor deposition (PVD) technique is well established as a method to elaborate a variety of coatings. In the last decades, a diversity of binary, ternary, and quaternary coatings were developed (Ref 1-3). CrN coatings exhibit interesting properties such as a good chemical stability, or wear and corrosion resistance (Ref 4, 5).

The incorporation of aluminum into the CrN system has a main influence on the films properties. Chim et al. (Ref 6) studied the oxidation resistance of CrN and CrAlN coatings synthesized by lateral rotating cathode arc. They found that the CrAlN coating had a better oxidation resistance than the CrN one. Moreover, the CrAlN hardness was higher (35 GPa) than the CrN (20 GPa) one. These results are also found by Barshilia et al. (Ref 7) using reactive direct current (DC) magnetron sputtering. They observed a hardness of about 33 GPa and 18 GPa for CrAlN and CrN, respectively, and a higher corrosion resistance for the CrAlN coating. Spain et al. (Ref 8) developed CrN, TiN, TiAlN, and CrAlN coatings by twin electron beam plasma assisted physical vapor deposition (EBPAPVD). Among all these coatings, CrAlN presents the best wear resistance.

Since 1980s, multilayer coatings have been intensively investigated due to their high wear resistance compared to the single layer coatings (Ref 9-12). This is due to the presence of interfaces between the different layers (Ref 13), which prevent the cracks propagation (Ref 14). It also prevents the dislocations slip which lead to an increase of the film hardness (Ref 15). A variety of hard multilayers coatings have been studied such as TiN/CrN (Ref 16), TiAlN/MoN (Ref 15), CrVN/TiN (Ref 17), etc.

Chen et al. (Ref 18) developed multilayer coatings of CrAlN/TiN and CrAlN/ZrN with a commercial cathodic arc evaporation system. In comparison to CrAlN/ZrN, CrAlN/TiN system shows a coherent interface and higher thermal and mechanical properties. Nose et al. (Ref 19) developed CrAlN/BN multilayer coatings by direct current (DC) and radio-frequency (RF) reactive magnetron sputtering. They showed that multilayer coatings exhibited higher oxidation resistance after an annealing for 1 hour in air at 800 °C compared to the CrAlN monolayer coatings: CrAlN/BN hardness remained stable, while the hardness of CrAlN decreased. The use of multilayer system also improved the tribological properties. Wang et al. (Ref 20) developed a multilayer coatings of CrAlN/VN by RF magnetron sputtering and showed that the multilayer coating tested against an Al2O3 ball at 700 °C using a ball-on-disk tribometer has the lowest coefficient of friction and wear rate compared to CrAlN and VN monolayers. The use of the multilayer system improves the hardness of the coatings. For example, the hardness of CrAlN coatings (27.1 GPa) slightly increased to 31.6 GPa with a multilayer coating of CrAlN/SiN (Ref 21). Maksakova et al. (Ref 22) developed a special coating architecture deposited by arc-PVD. They used multilayer nanostructured in each modulation period composed of 40 nitride bilayers CrN/ZrN and seven metallic bilayer Cr/Zr. They

Khalil Aouadi and **Moez Chafra**, Applied Mechanics and Systems Research Laboratory (LR03ES06), Tunisia Polytechnic School, University of Carthage, Rue El Khawarizmi, BP 743, 2078 La Marsa, Tunisia; **Corinne Nouveau** and **Aurélien Besnard**, Arts et Metiers Institute of Technology, LaBoMaP, Rue Porte de Paris, 71250 Cluny, France; **Brahim Tlili**, Ecole Nationale d'Ingénieurs de Tunis, Laboratoire de Mécanique Appliquée et Ingénierie (LR-MAI), Université de Tunis El-Manar, Rue Béchir Salem Belkhiria, 1002 Tunis, Tunisia; **Alex Montagne**, Arts et Metiers Institute of Technology, MSMP, 8, Rue Boulevard Louis XIV, 59046 Lille Cedex, France. Contact e-mail: aouadikhalil@hotmail.com.

note that multilayer showed a significantly higher hardness than that of monolayers CrN and ZrN. Also, CrN/ZrN films presented a reduced elastic modulus, and a higher value of resistance to plastic deformation and elastic strain to failure. Postolnyi et al. (Ref 23) have been studied CrN/MoN multilayer coatings fabricated by Arc-PVD. They studied the effect of bilayer thickness on the properties of CrN/MoN films. They showed that the structure changed with the decrease of the bilayer thickness because the grain size decrease and this leads to the Hall–Petch strengthening of films and to the blocking of cracks and dislocation propagation which enhance mechanical properties. Pogrebnjak et al. (Ref 24) developed of CrN/MoN fabricated by vacuum-arc evaporation. They studied the effect of periodically changing architecture of monolayers and varying the substrate bias voltage and nitrogen pressure. They noted that the decrease of nitrogen pressure causes a decrease of the tribological properties. Also, the decrease of the layers thickness leads to decrease of crystallite sizes. Multilayer hardness reaches 42 GPa with the decrease of individual layer thickness, and this is explained by the Hall–Petch strengthening mechanism.

The aim of the present work is to study CrN/CrAlN multilayer coatings using an industrial DC reactive magnetron sputtering system with different bilayers periods. The effect of the increase of the number of interfaces on the microstructure, surface morphology, mechanical, and tribological properties of CrN/CrAlN multilayer films is studied.

2. Experimental

2.1 Coatings Deposition

The CrN/CrAlN multilayer coatings with various bilayer thickness were synthesized by DC reactive magnetron sputtering (KENOSISTEC-KS40V). The diameter of the chamber is about 730 mm, its height is about 790 mm and its volume is about 340 L. The substrates are X50CrMoV8-1 steel samples ($20 \times 20 \times 5$ mm^3) and mirror polished silicon (100) (10×10 mm^2) 380 µm thick. The mass percent composition of X50CrMoV8-1 steel was examined using spark spectrometry and it described in Table 1.

Two targets of chromium and aluminum with purity of 99.95% and dimensions of 406.4×127 mm^2 with a thickness of 7.5 mm were used. Before deposition, all substrates were ultrasonically cleaned in acetone and alcohol for 5 min, respectively, and then dried under compressed air. Prior to the deposition, the chamber has been pumped down to a residual pressure of around 2.10^{-5} Pa at a temperature of 300 °C for 7 h. The input power on Cr and Al targets has been fixed at 1500 W and 1000 W, respectively. During deposition, the working pressure was fixed at 0.5 Pa. The flow rates of Ar and N2 were 68.8 and 33.3 sccm, respectively. The thickness of CrN and CrAlN underlayers was controlled by the deposition time. A substrate bias voltage of − 500 V was employed for all depositions. This value was optimized for CrN coating in a previous study (Ref 5). The substrate holder rotation was fixed at 1.5 rpm. Before deposition, all substrates were in situ etched under argon plasma at − 700 V for 10 min to remove contaminants and to ensure a better adhesion of the coatings.

Table 1. Chemical composition of X50CrMoV8-1 steel using spark spectrometry

% C	% Cr	% Mn	% Si	% V	% Mo	% Fe
0.5	8	0.5	1	0.5	1.5	88

The total thickness of multilayer coatings was around 2 µm. We chose to study the effect of interfaces on the CrN/CrAlN films properties. We chose a bilayer number of 1, 2, 3, and 4. That's why we chosed the following values of 1000, 500, 350, 250, and 200 nm. The top layer for each multilayer coating is always CrAlN and a chromium underlayer of about 120 nm was systematically realized. Figure 1 presents the different types of multilayer coatings studied. Five multilayer coatings are realized (C1, C2, C3, C4, C5) with different number of interfaces (1, 2, 3 and 4). For C5, we choose to developed a multilayer coating with a thickness gradient choosing the same layer thicknesses used in the other coatings (1000, 500, 250) and keeping the total thickness (∼ 2000 nm).

2.2 Characterizations of the Coatings

The surface morphology and the microstructure of the coatings were observed by HR-SEM (JEOL JSM 7610F). The chemical composition of coatings and of wear tracks after ball-on-disk tests were determined by energy-dispersive x-ray spectroscopy (EDS) and wavelength dispersive spectroscopy (WDS) analysis (JEOL JSM 6400F). The crystallinity of the films was characterized by x-ray diffraction (XRD) (INEL diffractometer type curve CPS 120 detector, Kα Co radiation source of 0.178897 nm) with a voltage of 25 kV and a current of 25 mA at low angle configuration (5°). The coherent domain sizes were calculated by Scherrer's equation (Eq 1):

$$d = \frac{K * \lambda}{\beta * \cos\theta}, \quad \text{(Eq 1)}$$

where K is the Scherrer's constant (0.9 in our case), λ is the x-ray wavelength, β is the broadening of the full width at the half maximum (FWHM) and θ is the Bragg's angle. The coherent domain sizes are calculate from the main peak.

The friction coefficient was measured by rotative ball-on-disk tests in ambient air under a fixed load of 5 N, a sliding speed of 3 cm/s and for a sliding time of 65 min, using an alumina ball (6 mm of diameter) as counterpart. After the ball-on-disk tests, the wear volumes were evaluated from optical profilometer (VEECO, Wyko-NT 1100) profiles at eight different positions in the wear track (each 45°). Surface morphology was analyzed by Atomic Force Microscopy (AFM, type XE sPark 70) using tapping mode with a scanning area of 5×5 µm^2. Gwyddion software was used to calculate the coating roughness. The hardness and Young's modulus were determined by nano- indentation tests using a MTS XP Nano-indenter equipped with a Berkovich indenter. The tip radius of the indenter is about 200 µm, and it face angle is about 136°. The maximum load is about 750 mN. To calculate the hardness, Rahmoun's model (Ref 25) was used. Scratch tests were performed on Scratch Tester Millennium 200 equipped with a Rockwell spherical diamond indenter (with tip radius of 200 µm and a conical angle of 120°) with a continuous increase of the normal load from 0 to 200 N and equipped with acoustic emission detector. The scratch length is about 8 mm. For each coating, three tests are realized and an average adhesion value of Lc2 is calculated. The residual stress

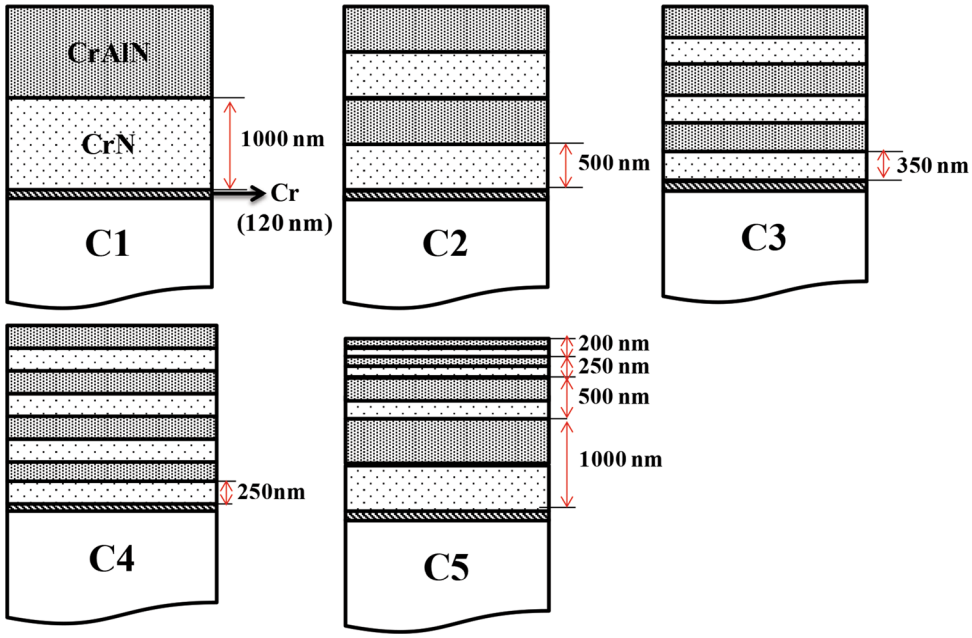

Fig. 1 Scheme of the multilayer systems

in all thin films was evaluated using the modified Stoney formula (Eq 2) (Ref 5):

$$\sigma = \frac{E_S}{6(1-\nu_S)}\frac{e_S^2}{e_f}\left(\frac{1}{R}\right) - \left(\frac{1}{R_0}\right), \qquad \text{(Eq 2)}$$

where E_S: Young's modulus of the substrate, versus: Poisson's ratio of the substrate,e_s: substrate thickness, *ef*: film thickness, *R*: radius of curvature after deposition and *R*0: radius of curvature before deposition. The radiuses of curvature (*R*0 and *R*) are determined by 3D optical profilometer (VECCO, Wyko-NT 1100).

3. Results and Discussion

3.1 Physico-Chemical Properties

In Fig. 2, the column size is shown and it determined by (Scanning Electron Microscopy) SEM.

The quantitative chemical composition of CrN and CrAlN monolayers obtained by EDS analysis are listed in Table 2. One can note that CrN and CrAlN coatings exhibit a low oxygen concentration. The existence of this amount of oxygen may be ascribed to the residual oxygen into the chamber. It can be shown that the as-deposited CrN coating presents the stoichiometric concentration ratio with a N/Cr ratio of 0.96. 7% of Al were inserted to produce CrAlN films with an optimized Al/(Al+Cr) ratio of 0.14.

Figure 3 depicts the XRD patterns of each CrN and CrAlN monolayers and CrN/CrAlN multilayer coatings deposited with various bilayer periods.

In comparison with the standard reference sample listed in (ICCD96-431-1895 and 96-153-5441) PDF database, the CrN monolayer coating presents characteristic diffraction peaks at 43°, and 75.17° corresponding to (111) and (202) planes of fcc cubic structure, respectively. CrN shows a (111) preferential orientation. CrAlN monolayer also has the fcc structure with similar peaks to that of CrN coating with a weak (111) peak. In addition, peak at 51.09° corresponding to CrN (200) plan appears.

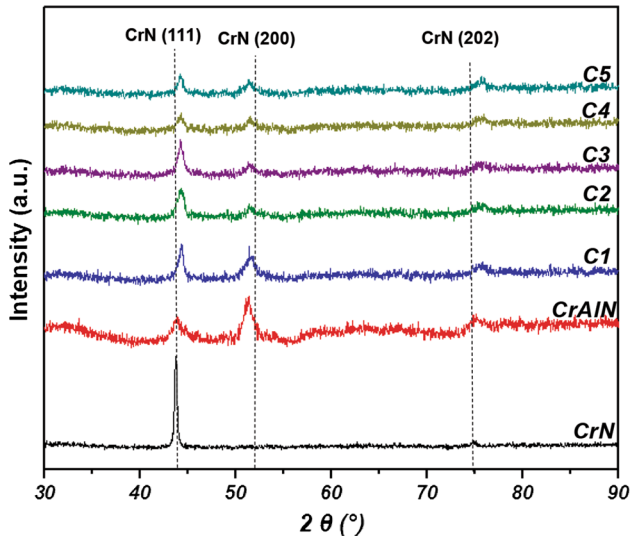

Fig. 2 SEM cross-sectional image of CrN/CrAlN (C1)

Table 2. Chemical composition of CrN and CrAlN monolayer coatings obtained by EDS and WDS analysis

	Composition, at.%			
	N	O	Cr	Al
CrN	46.8	4.8	48.4	–
CrAlN	46.4	4.6	41.9	7.1

The decrease of the (111) diffraction peak is ascribed to the incorporation of Al. This is due to the lattice distortion caused by the addition of Al atoms. On the other hand, varying the number of bilayer periods has no obvious influence on the XRD patterns. The detected peaks of all multilayer coatings coincide well with the CrAlN single layer. No AlN phases are detected in all coatings. This result can be explained by the fact that Al atoms exist as amorphous nitride phase or incorporate in the fcc lattice or both. Besides, this can be due to the high ratio of Cr/Al (Ref 26). As the number of bilayer increases, the intensity of CrN (111) and CrN (200) peaks decreases, indicating that the coherent domain size gradually reduces (Ref 27, 28). This is consistent with results presented in Table 3. Also, this decrease of the intensity of CrN (111) and CrN (200) peaks can be ascribed to the decrease of bilayer thickness (Ref 29).

CrN (200) diffraction peaks of the multilayers are shifted to higher angles compared to the same planes in the CrAlN monolayer. Kim et al. (Ref 30) attributed this result to higher residual stresses in multilayer coatings. Bouaouina et al. (Ref 31) who deposited multilayers coatings of Mo2N/CrN by RF magnetron sputtering explain this phenomenon by the decrease of residual stress caused by interfaces between Mo2N and CrN. According to the Bragg's equation ($2.d.\sin(\theta) = n.\lambda$, where n and λ are two constants), the diffraction peaks will be shifted if there are compressive or tensile stresses (Ref 15). On the other hand, we observe that the peak intensity of CrN (111) decreases with the increase of bilayers. This can be explained by the decrease of coherent domain size as shown in Table 3.

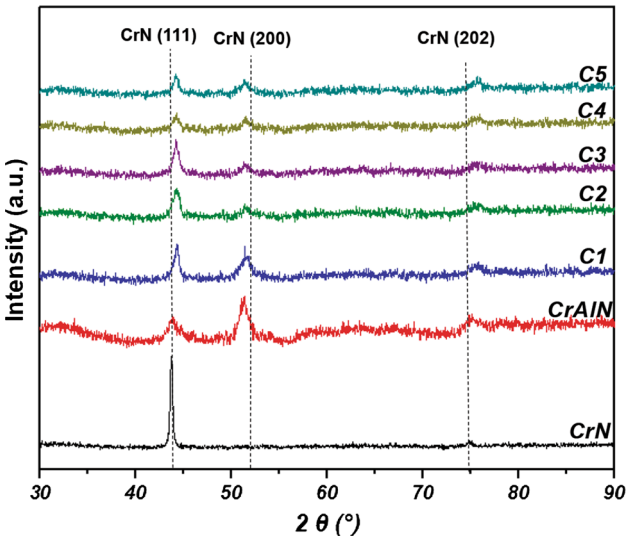

Fig. 3 XRD patterns of CrN/CrAlN multilayer coatings

Figure 4 illustrates the SEM fracture cross section of CrN/CrAlN multilayer coatings with different bilayer thickness on Si substrates. All multilayer coatings CrN/CrAlN present a columnar structure. The Cr underlayer is clearly observed in contact with the substrates. It is deposited to improve the adhesion strength and reduce the internal stress between substrate and CrN/CrAlN multilayer coating. From this metallic fine grain underlayer, the columns tend to become larger and then remain constant in size along the film thickness. The thickness values of all multilayer films are around 2 μm. Multilayer coating with only one bilayer (C1) has the widest columns while films C4 and C5 have the thinnest columns. This is confirmed by the column size in Table 3.

AFM surface morphologies images of CrN/CrAlN multilayer coatings deposited with different bilayer thickness are presented in Fig. 5.

To exhibit the AFM images, a $5 \times 5\ \mu m^2$ area were used to determine the RMS roughness and column size (Table 3). RMS roughness values as a function of bilayer number are listed in Table 3. By varying the number of bilayers from 1 to 4, roughness of the surface decreases from 34.9 to 22.5 nm. Similar results have been obtained by other researchers (Ref 15, 31). This indicates that multilayer coating with one bilayer grow more disordered than multilayer with 4 bilayers. This reduction of the roughness as the number of bilayers increases may be due to the decrease of coherent domain size (Table 3). Indeed, the coherent domain size value of multilayer coatings reduces with the increase of the bilayer period and reaches 8.2 nm for C5 multilayer coating which implies that the variation of bilayer period greatly affects the coherent domain size. This is attributed to the decreasing of the individual thickness for each interlayer when the bilayer period is increased. Thus, this leads to a decrease of the total surface roughness (Ref 32).

3.2 Mechanical Properties

In Table 4 are presented the hardness, Young's modulus, H/E and H^3/E^{*2} of the different films studied. H/E ratio represents the elastic strain failure. When this ratio is large, the propagation of the force takes more time which delay the failure of films (Ref 33). From Table 4, it can be seen that elastic strain failure values of CrN and CrAlN monolayer films were the lowest. This indicates that the multilayer structure enhances the elastic strain failure. Moreover, with the increasing of the number of bilayers, H/E ratio increases from 0.096 for C1 to 0.106 for C5 coating. This is with a good correlation with results obtained by Postiolnyi et al. (Ref 23) whose confirm that elastic strain failure increase when the bilayer thickness decrease.

The H^3/E^{*2} ratio ($E^*=E/(1-\nu^2)$) which represents the plastic deformation resistance of materials is also shown in

Table 3. Coherent domain size, thickness and column size of CrN/CrAlN multilayer coatings

Specimen	Coherent domain size, nm	Column size, nm	RMS roughness, nm
C1	18.6 ± 0.4	61	34.9
C2	16.8 ± 0.3	56.4	32.3
C3	14.4 ± 0.4	50	30.8
C4	12.1 ± 0.5	38	22.5
C5	8.2 ± 0.6	31.6	27.5

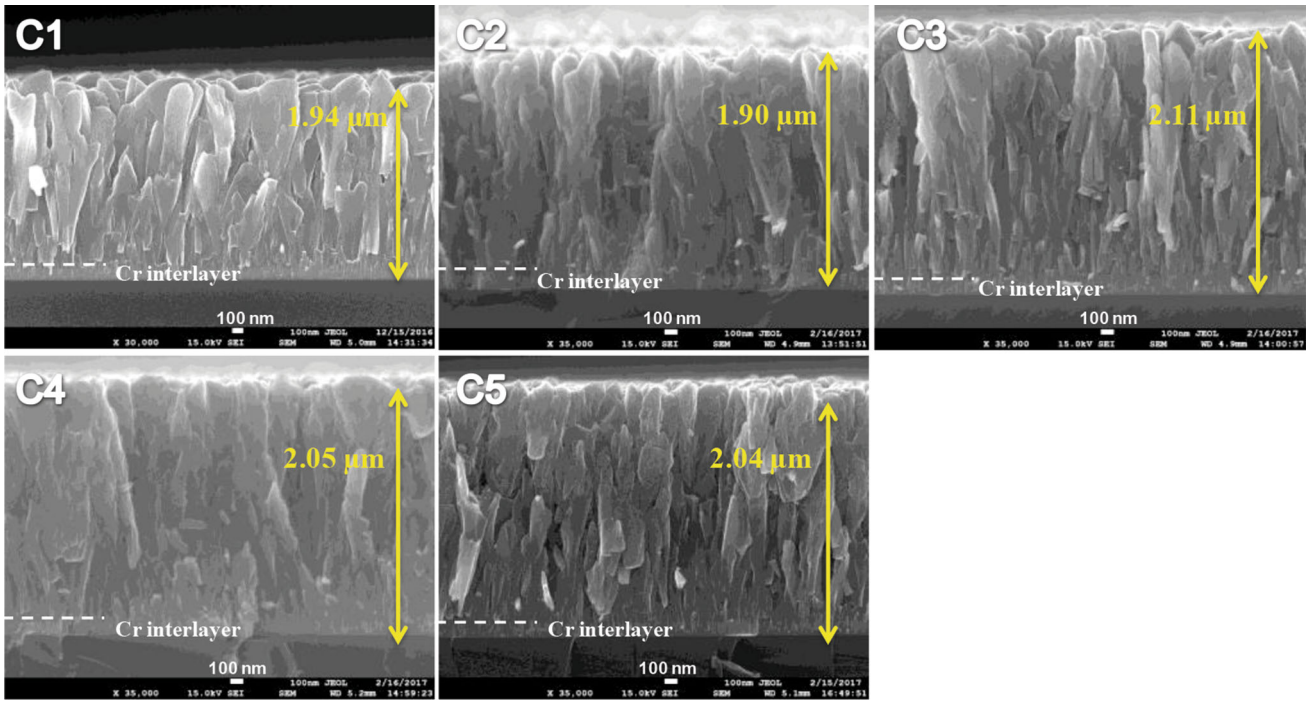

Fig. 4 SEM cross-sectional images of CrN/CrAlN multilayer coatings

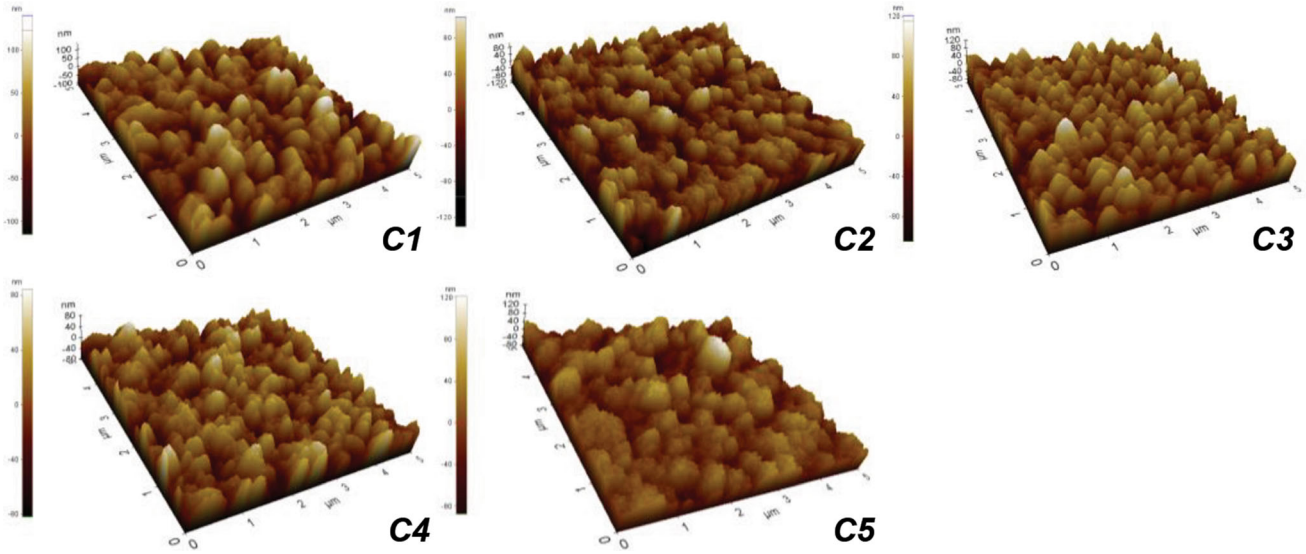

Fig. 5 AFM images of CrN/CrAlN coatings

Table 4. Mechanical properties of the studied coatings

	Hardness, GPa	Young's Modulus, GPa	H/E	H^3/E^*2	Residual stress, MPa
CrN	22 ± 0.9	244 ± 6.0	0.090	0.164	86.4
CrAlN	27 ± 1.0	305 ± 5.0	0.088	0.194	296
C1	35 ± 0.8	361 ± 5.0	0.096	0.303	261
C2	37 ± 1.0	372 ± 6.0	0.099	0.337	236
C3	40 ± 0.7	392 ± 4.5	0.102	0.383	220
C4	39 ± 1.1	380 ± 6.0	0.102	0.378	193
C5	43 ± 0.7	402 ± 5.5	0.106	0.453	171

Table 4. The CrN/CrAlN multilayer coatings exhibit higher H^3/E^{*2} ratio than CrN and CrAlN monolayer films. It is also obvious that the plastic deformation of the multilayer coatings increases with the number of bilayers and C5 film presents the highest plastic deformation resistance. This is due to the higher number of interfaces between bilayers, thus the crack propagation is delaying and the toughness of coatings enhanced (Ref 26).

The hardness and Young's modulus of the CrN, CrAlN coatings and the CrN/CrAlN multilayer coatings as a function of bilayers periods are illustrated in Fig. 6.

The results show that hardness and Young's modulus of CrN/CrAlN films are influenced by the bilayers period. Indeed, the hardness and Young's modulus of CrN/CrAlN multilayer increase with the increase of the number of bilayers from 35 to 43 GPa for the hardness and from 361 to 402 GPa for the Young's modulus. Multilayer coating with four bilayers and different thickness (C5) presents the highest coating hardness (43 GPa) which is a worthy value. The coatings hardness increases with the decrease of the bilayer period thickness. This is confirmed by the literature where it has be proved that there is a correlation between the period thickness and the multilayers hardness (Ref 23, 34, 35). The hardness of the CrN and CrAlN monolayers are, respectively, 22 and 27 GPa which are lower than that of multilayers coatings. These results are in a good correlation with other studies (Ref 15, 36-38). The increase of hardness and Young's modulus of the multilayers can be explained by the decrease of each monolayer thickness and the use of multilayer coatings with thicknesses of few decade or hundred nanometers. Indeed, microstructure depends on the bilayers size of period which generates the improvement of mechanical properties (Ref 32). The increase of the modulation period of multilayer leads to the decrease of the coherent domain size, as observed from Table 3, causes an increase of the film density (Ref 39). The high density of multilayer coatings inhibits dislocation motion across interfaces. In other words, this enhancement of hardness can be due to the refinement of films grain size (Table 3). Indeed, the decrease of the grain size has a main effect on the improvement of coatings hardness according to the Hall–Petch's relation (Ref 40) where each interface acts as a grain boundary (Ref 41). The decrease of grain size can encourage the pile-up of dislocation and blocks the dislocation motion. In fact, smaller grain sizes lead to smaller void at interfaces which prevents dislocation slip. Then, dislocations are hindered at monolayers under the effect forces generated from the two monolayers like dislocations pile-up (Ref 42). This is having a positive influence on the hardness increasing. Pogrebnjak et al. (Ref 24) explain the increase of multilayer hardness with the decrease of monolayers thickness by the reduction of grain size because the growth of grain boundary volume prohibits the dislocation sliding. Dislocations pile-up at interfaces can strengthen coatings and then improve coatings hardness. According to Barnett et al. (Ref 43), the difference in layer elastic modulus is an important factor in determining the hardness improvement. In addition, there is a strong relationship between the nature of interface and the enhancement in hardness (Ref 44, 45). Indeed, smooth and sharp interface can block the movement of dislocations and then promotes the enhancement of the hardness.

The increase in the number of bilayers to 4 is accompanied by a slight decrease of the hardness and Young's modulus. The coherent grain size of this multilayer coating (C4) is smaller than that of the film with three bilayers (Table 3). However, its hardness is 39 GPa and its Young's modulus is about 381 GPa. Indeed, not only the grain size, but also the inter-diffusion and the state of interface layered must be taken into account to explain the evolution of hardness, Young's modulus and their dependence on the process parameters (Ref 15).

Figure 7 shows the critical loads of the CrN/CrAlN films as a function of the number of bilayers periods.

Critical load of CrN/CrAlN multilayer coatings were presented in term of Lc2 which represent the critical load for the continuous cracking. We observe that critical load values of multilayer coatings are greater than those of monolayers (CrN and CrAlN). It can be seen that the bilayer thickness greatly affects the adhesion strength. Indeed, for a single period, critical load is about 74 N while a bilayer periods of 4 (C5) has an Lc2 equal to 97 N, which indicates an excellent adhesion. This result can be explained by the increase of plasticity (Ref 15). Besides, the enhancement of the adhesion strength behavior of the multilayer coatings can be attributed to the micro-cracks developed initially at the top surface. Each interface can greatly change the direction of the initial crack during its penetration into the coatings, delaying cracks propagation. Therefore, multilayer structure permits to improve mechanical properties thanks to the different interfaces that

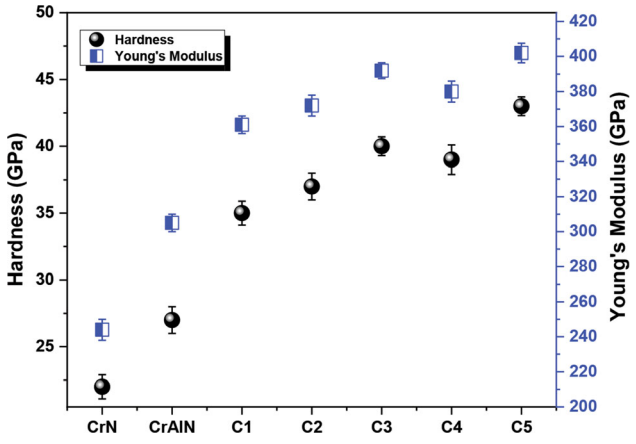

Fig. 6 Hardness and Young's modulus of CrN, CrAlN and CrN/CrAlN multilayer coatings

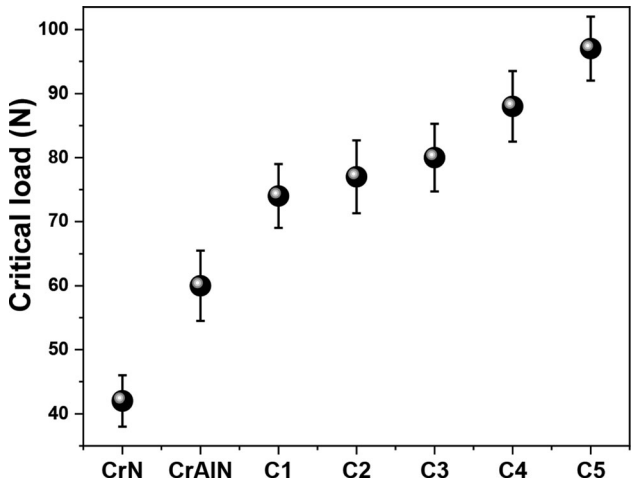

Fig. 7 Critical load of CrN, CrAlN and CrN/CrAlN multilayer coatings as a function of bilayer periods

prevent the dislocations motion. Besides, with the decrease of the bilayer thickness, the dislocations that exist in layers constitute a major obstacle to move. Hence, this requires a higher critical shear stress to propagate and move across the whole coating and cause the delamination of the multilayer coating (Ref 46, 47). According to Zhang et al. (Ref 48), this increase in critical load (Lc2) can be attributed to the increase of H/E^* value which represents the resistance to cracking. This is in good correlation with results shown in Table 4. The two films with 4 bilayer periods have the same number of interfaces but, the coating with periods of different thicknesses (C5) has a better resistance adhesion. This can be explained by the better hardness and wear resistance of C5 (Fig. 6).

For the multilayer coatings, it can be seen that when the tensile stress is low, the adhesion is better (Table 4). In general, the curvature and deformation of thin films are provoked by tensile stress. This phenomenon can create a bending moment at the coating/substrate interface. Meantime, the bending moment direction is toward the coating and this can easily induce the debonding of interfaces (Ref 28).

3.3 Tribological Properties

Figure 8 shows the coefficient of friction (COF) of CrN, CrAlN and CrN/CrAlN multilayer coatings deposited with different bilayer periods versus the sliding distance.

The coefficient of friction behavior for multilayer coatings presents two distinct steps: first, there is the runin step, where the COF increases progressively resulting from the rough surface, contaminants, and the contact stress variation. Afterward, the COF stabilizes and remains constant until the end of the test. It can be observed that the friction behavior of CrN monolayer becomes stable after the shortest distance (~ 10 m), while multilayer coatings take the longest distance (~ 30 m) before their stabilization. The average value of the multilayer coatings COF is 0.68. The COF for multilayer coatings is lower than that of CrAlN monolayer which is around 0.8 but higher than that of CrN which is around 0.51. This is in correlation with the literature where the COF of multilayer coatings is between that of monolayers (Ref 17, 49).

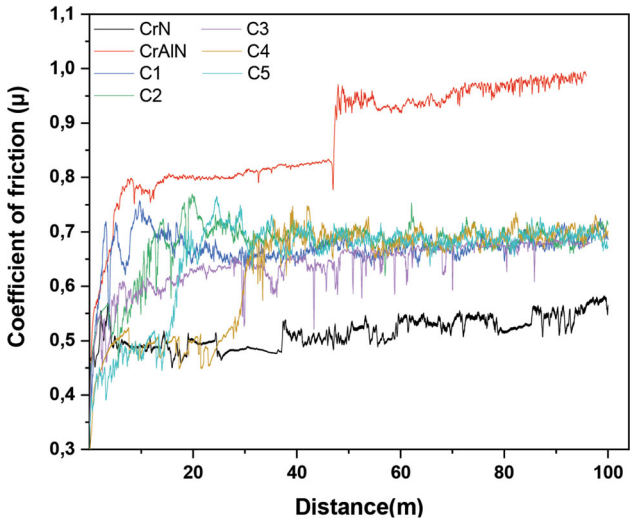

Fig. 8 Friction coefficient of CrN and CrAlN monolayer coatings and the CrN/CrAlN multilayer with different bilayer periods

The wear volume was calculated after the ball-on-disk tests. Fig. 9(a) shows the wear volume of the coatings studied.

All CrN/CrAlN multilayer coatings show a wear volume lower than that of CrN and CrAlN monolayers (Fig. 9). This result is in correlation with Fig. 6: the hardest the coating is, lower the wear volume. Indeed, under the same conditions, we noted that the wear volume of the CrAlN film is 1.22×10^{-5} mm^3 and that of the CrN is 1.64×10^{-5} mm^3. The wear volumes of the multilayer coatings varied from 8.5×10^{-6} to 1.03×10^{-5} mm^3. This improvement of wear resistance can be associated to the increase of the material ability to resist to plastic deformation (H^3/E^{*2}) and the elastic strain failure (H/E) which can play a crucial role in the tribological behavior (Ref 28, 50) (Table 4). As a matter of fact, with a high plastic deformation resistance (H^3/E^{*2}), the external load can be dissipated over a wider elastic strained area which can enhance the wear resistance (Ref 48). As a consequence, a high H^3/E^{*2} leads to a reduced wear volume. In addition, the increase in the number of interfaces improves the tribological behavior of multilayer coatings (Ref 15). Interfaces interact with dislocations and crack propagation as follows: the greater the number of interfaces is, the greater the barriers of crack propagation, resulting in a better wear resistance. According to Zhou et al. (Ref 51), the wear resistance of TiN/CrN multilayer coatings decreases with the increase of the period thickness. They

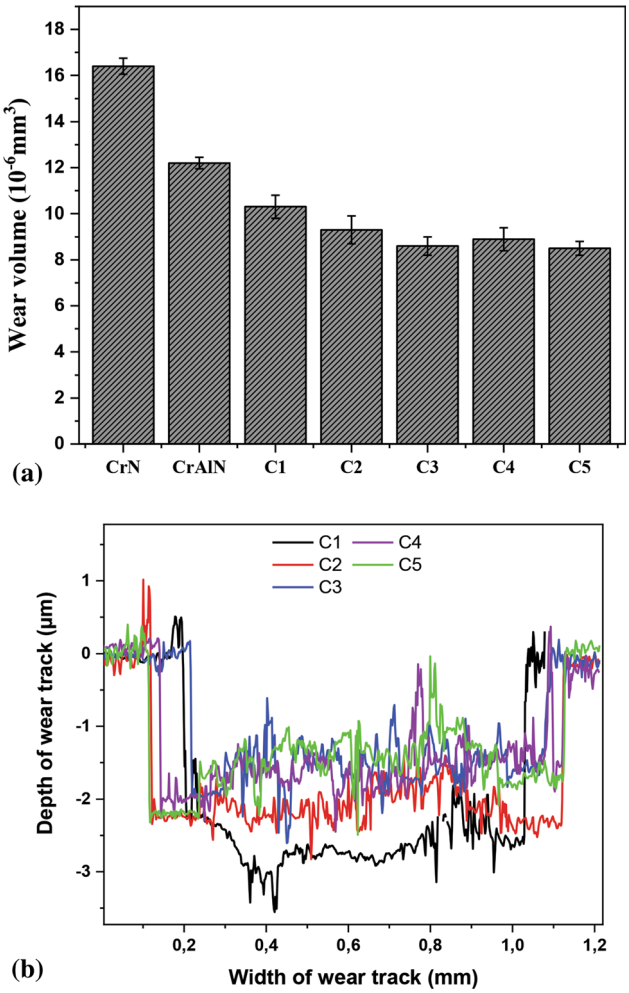

Fig. 9 Wear volume (a) and wear track profiles (b) of CrN/CrAlN multilayer coatings as a function of their number of bilayers

explained this result by the decrease of the anchoring energy into interfaces which generates delamination of layers, leading to the formation of debris and to the reduction of the wear resistance. So, the thicker the bilayer is, the lower the resistance wear. Likewise, this increase in the wear resistance can be attributed to the hardness enhancement. Indeed, high hardness can give rise to an increase load carrying capacity, less contact area with counterpart (Ref 52). Also, it is well known that hardness is inversely proportional to the wear rate (Ref 53).

Figure 9(b) exhibits wear track profiles of CrN/CrAlN multilayer coatings. The depth of wear track of C1 and C2 is higher than their coating thickness. Indeed, from Fig. 4, the coating thickness of C1 and C2 is 1.94 and 1.90 µm, respectively. However, their wear depth is higher than 2 µm. For C3, C4, and C5 multilayer coatings, the wear track depth is about 1.5 µm and their coating thickness is about 2.11, 2.05, and 2.04 µm, respectively, (Fig. 4) implying that these multilayer coatings are not worn out.

The wear tracks were observed by SEM and analyzed by EDS. The results are presented in Fig. 10. For all multilayer coatings, a narrow wear tracks are shown and no cracks are observed. Furthermore, all images of wear tracks showed a lamellar delamination of all multilayer coatings. From SEM images of C1 and C2 (Fig. 10a and b), it is obvious that these two coatings present a smooth wear track. These images combined to EDS profiles revealed that these coatings are totally delaminated and as a result, the substrate exposed. This is may be due to the low plastic deformation and to the low toughness of these coatings (Ref 54). Indeed, from Table 4, C1 and C2 present the lowest plastic deformation resistance H^3/E^{*2}. Also, the worn-out hard debris acted as a third-body abrasion against the alumina ball which leads to the substrate exposure (Ref 55, 56). This confirms the poor wear resistance of these two coatings as indicated in Fig. 9. In the case of C1 (Fig. 10a), numerous adherent debris are piled on the edge of wear track and scratches are shown along the sliding direction. However, grooves are not detected in the wear track which implies that the adhesive wear is promoted (Ref 57). In the C2 multilayer, one can note the existence of a white area in the middle of the wear track. This indicates that this area was oxidized. During dry sliding, a local high temperature is created and an oxide is formed after the reaction between the top layer and the oxygen of the ambient atmosphere. Also, the wear track of C2 presents a partial delamination on its edge.

For C3 and C4 multilayer coatings the wear track is constituted by Fe, Cr, and O which means that some traces of coating still remain in the wear tracks. This indicates that the intrinsic stress in the coating/substrate contact dominates over the contact stress existing between the sliding interfaces (Ref 58). Besides, this improvement of the wear resistance may be attributed to the enhancement of the fracture toughness (Ref 58). From Fig. 10(e), the wear track of the C5 coating is rich in Cr, Al, and N element, implying that the delamination may be only in the top layers. Also, it presents a severe spallation at the edge of the wear track. According to Ou et al. (Ref 16), crack initiation, delamination and wear debris are occurred due to the plastic and elastic deformation. The increase of the adhesion resistance of C3, C4, and C5 multilayer coatings during sliding tests is ascribed to the improved adhesion strength with the increase of the bilayer number. Thereby, improved adhesion strength and toughness with the increase of critical load of CrN/CrAlN multilayer coatings delay the coating delamination and wear debris formation. This is in good relationship with Fig. 7 and Table 4.

In the literature (Ref 54, 59, 60), it has been proved that in multilayer coatings structure various parameters can enhance toughness and mechanical properties: type of interlayers, number and thickness of each interlayer, multilayer design,

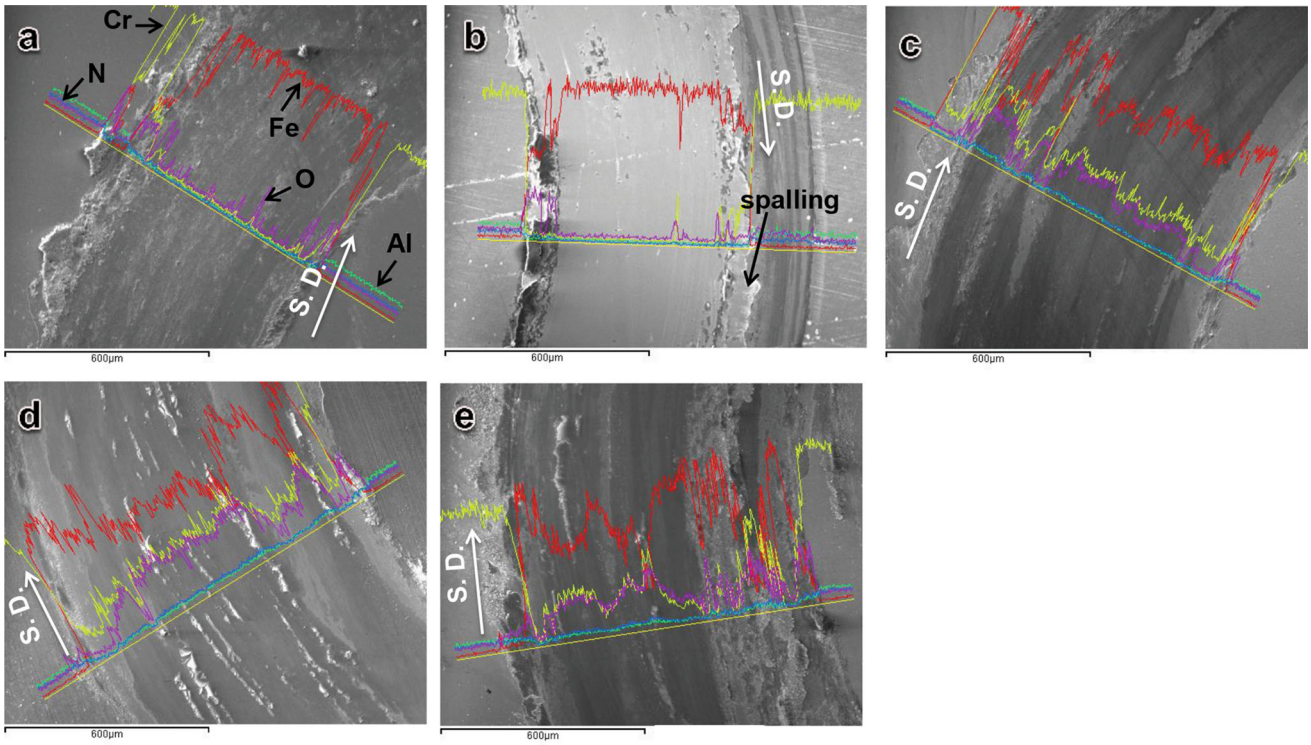

Fig. 10 SEM images and EDS analysis of wear track of (a) C1, (b) C2, (c) C3, (d) C4 and (e) C5 multilayer coatings

and the thickness ratio of different monolayers. In this study, the wear mechanism can be created by a ''layer by layer'' mechanism (Ref 61). The wear mechanism starts by the CrAlN top layer until the appearance of the fatigue cracks which can spread and reach CrAlN/CrN interface. Thus, the CrN layer is exposure to the wear mechanism. After the delamination of the CrN layer, a new CrAlN layer begins to wear and the process repeats.

4. Conclusions

In this study, CrN/CrAlN multilayer coatings with various bilayer thicknesses were obtained by DC magnetron sputtering on X50CrMoV8-1 stainless steel and (100) silicon substrates. The main objective of this research was to evaluate the effect of bilayer thickness on the microstructure, mechanical and tribological properties of the CrN-based multilayers. Our conclusions are as follows:

- XRD patterns of CrN/CrAlN multilayer coatings indicated that varying bilayer thickness has no effect on their structure or crystallinity. All detected diffraction peaks coincide with that of CrAlN monolayer. No AlN diffraction peaks were detected.
- SEM cross-sectional images exhibited that CrN/CrAlN layers deposited with various bilayer periods have a columnar structure with a smaller coherent domain size.
- All multilayer coatings exhibited better mechanical properties than that of monolayers. Especially, CrN/CrAlN film with four bilayers and different monolayers thickness possess the highest hardness (43 GPa), elastic modulus (402 GPa) and an excellent resistance to spallation (Lc2 up to 97 N).
- All multilayer coatings showed good tribological properties. CrN/CrAlN film with four bilayers and different monolayers thickness exhibits an optimal wear resistance which is ascribed to its good hardness and critical load (Lc2).

Overall results of this work indicate that CrN/CrAlN multilayer coating obtained with 4 bilayer and different monolayers thickness (C5) presented the best hardness and Young's modulus, the best adhesion, the lowest coherent grain size, the best plastic deformation resistance and the best wear resistance.

Acknowledgments

The authors would like to thank the Regional Council of Burgundy for its financial support. The authors also, would like to thank M. Denis LAGADRILLERE for the SEM observations and EDS microanalyses, Dr. Philippe JACQUET for the XRD analyses. We also think Pr. Alain IOST and Dr. Alberto MEJIAS for their help in nanoindentation and scratch test measurements.

References

1. L. Aihua, D. Jianxin, C. Haibing, C. Yangyang and Z. Jun, Friction and Wear Properties of TiN, TiAlN, AlTiN and CrAlN PVD Nitride Coatings, *Int. J. Refract. Met. H.*, 2012, **31**, p 82–88
2. H. Elmkhah, T. Zhang, A. Abdollah-zadeh, K. Kim and F. Mahboubi, Surface Characteristics for the Ti-Al-N Coatings Deposited by High Power Impulse Magnetron Sputtering Technique at the Different Bias Voltages, *J. Alloys Compd.*, 2016, **688**, p 820–827
3. H. Du, J. Xiong, H. Zhao, Y. Wu, W. Wan and L. Wang, Structure and Properties of TiAlLaN Films Deposited at Various Bias Voltages, *Appl. Surf. Sci.*, 2014, **292**, p 688–694
4. T. Polcar, N.M.G. Parreira and R. Novák, Friction and Wear Behaviour of CrN Coating at Temperatures up to 500 °C, *Surf. Coat. Technol.*, 2007, **201**, p 5228–5235
5. K. Aouadi, B. Tlili, C. Nouveau, A. Besnard, M. Chafra and R. Souli, Influence of Substrate Bias Voltage on Corrosion and Wear Behavior of Physical Vapor Deposition CrN Coatings, *J Mater. Eng. Perform.*, 2019, **28**, p 2881–2891
6. Y.C. Chim, X.Z. Ding, X.T. Zeng and S. Zhang, Oxidation Resistance of TiN, CrN, TiAlN and CrAlN Coatings Deposited by Lateral Rotating Cathode Arc, *Thin Solid Films*, 2009, **517**, p 4845–4849
7. H.C. Barshilia, N. Selvakumar, B. Deepthi and K.S. Rajam, A Comparative Study of Reactive Direct Current Magnetron Sputtered CrAlN and CrN Coatings, *Surf. Coat. Technol.*, 2006, **201**, p 2193–2201
8. E. Spain, J. Avelar-Batista, M. Letch, J. Housden and B. Lerga, Characterisation and Applications of Cr-Al-N Coatings, *Surf. Coat. Technol.*, 2005, **200**, p 1507–1513
9. X. Xu, F. Su and Z. Li, Tribological Properties of Nanostructured TiAlN/W2N Multilayer Coating Produced by PVD, *Wear*, 2019, **430–431**, p 67–75
10. S. Huang, C. Tong, T. Hsieh and J. Lee, Microstructure and Mechanical Properties Evaluation of Cathodic arc Deposited CrCN/ZrCN Multilayer Coatings, *J. Alloys Compd.*, 2019, **803**, p 1005–1015
11. H.C. Barshilia, A. Jain and K.S. Rajam, Structure, Hardness and Thermal Stability of Nanolayered TiN/CrN Multilayer Coatings, *Vacuum*, 2004, **72**, p 241–248
12. M. Nordin, M. Larsson and S. Hogmark, Mechanical and Tribological Properties of Multilayered PVD TiN/CrN, TiN/MoN, TiN/NbN and TiN/TaN Coatings on Cemented Carbide, *Surf. Coat. Technol.*, 1998, **106**, p 234–241
13. P. Wiecinski, J. Smolik, H. Garbacz, J. Bonarski, A. Mazurkiewicz and K.J. Kurzyd, Microstructure and Properties of Metal/Ceramic and Ceramic/Ceramic Multilayer Coatings on Titanium Alloy Ti_6Al_4V, *Surf. Coat. Technol.*, 2017, **309**, p 709–718
14. P. Wiecinski, J. Smolik, H. Garbacz and K.J. Kurzydlowski, Erosion Resistance of the Nanostructured Cr/CrN Multilayer Coatings on Ti_6Al_4V Alloy, *Vacuum*, 2014, **107**, p 277–283
15. M. Yousaf, V. Pelenovich, B. Yang, C.S. Liu and D.J. Fu, Effect of Bilayer Period on Structural and Mechanical Properties of Nanocomposite TiAlN/MoN Multilayer Films Synthesized by Cathodic Arc Ion-Plating, *Surf. Coat. Technol.*, 2015, **282**, p 94–102
16. Y. Ou, J. Lin, H. Che, W. Sproul, J. Moore and M. Lei, Mechanical and Tribological Properties of CrN/TiN Multilayer Coatings Deposited by Pulsed DC Magnetron Sputtering, *Surf. Coat. Technol.*, 2015, **276**, p 152–159
17. E. Contreras, Y. Galindez, M.A. Rodas, G. Bejarano and M.A. Gómez, CrVN/TiN Nanoscale Multilayer Coatings Deposited by DC Unbalanced Magnetron Sputtering, *Surf. Coat. Technol.*, 2017, **332**, p 214–222
18. L. Chen and Y.X. Xu, Influence of Interfacial Structure on the Mechanical and Thermal Properties of CrAlN/ZrN Multilayer Coatings, *Mater. Des.*, 2016, **106**, p 1–5
19. M. Nose, T. Kawabata, T. Watanuki, S. Ueda, K. Fujii, K. Matsuda and S. Ikeno, Mechanical Properties and Oxidation Resistance of CrAlN/BN Nanocomposite Coatings Prepared by Reactive DC and RF Cosputtering, *Surf. Coat. Technol.*, 2011, **205**, p 33–37
20. Y. Wang, J. Lee and J. Duh, Mechanical Strengthening in Self-lubricating CrAlN/VN Multilayer Coatings for Improved High-temperature Tribological Characteristics, *Surf. Coat. Technol.*, 2016, **303**, p 12–17
21. C. Lin, Y. Tsai and J. Duh, Effect of Grain Size on Mechanical Properties in CrAlN/SiNx Multilayer Coatings, *Thin Solid Films*, 2010, **518**, p 7312–7315
22. O. Maksakova, R. Webster, R. Tilley, V. Ivashchenko, B. Postolnyi, O. Bondar, Y. Takeda, V. Rogoz, R. Sakenova, P. Zukowski, M. Opielak, V. Beresnev and A. Pogrebnjak, Nanoscale Architecture of (CrN/ZrN)/(Cr/Zr)Nanocomposite Coatings: Microstructure, Composition,

Mechanical Properties and First-Principles Calculations, *J. Alloys Compd.*, 2020, **831**, p 154808
23. B. Postolnyi, V. Beresnev, G. Abadias, O. Bondar, L. Rebouta, J. Araujo and A. Pogrebnjak, Multilayer Design of CrN/MoN Protective Coatings for Enhanced Hardness and Toughness, *J. Alloys Compd.*, 2017, **725**, p 1188–1198
24. A. Pogrebnjak, V. Beresnev, O. Bondar, B. Postolnyi, K. Zaleski, E. Coy, S. Jurga, M. Lisovenko, P. Konarski, L. Rebouta and J. Araujo, Superhard CrN/MoN Coatings with Multilayer Architecture, *Mater. Des.*, 2018, **153**, p 47–59
25. K. Rahmoun, A. Iost, V. Keryvin, G. Guillemot and N. Sari, A Multilayer Model for Describing Hardness Variations of Aged Porous Silicon Low-Dielectric-Constant Thin Films, *Thin Solid Films*, 2009, **518**, p 213–221
26. G. Li, J. Sun, Y. Xu, Y. Xu, J. Gu, L. Wang, K. Huang, K. Liu and L. Li, Microstructure, Mechanical Properties, and Cutting Performance of TiAlSiN Multilayer Coatings Prepared by HiPIMS, *Surf. Coat. Technol.*, 2018, **353**, p 274–281
27. W. Dai, Q. Wang, K. Kim and S. Kwon, Al_2O_3/CrAlSiN Multilayer Coating Deposited Using Hybrid Magnetron Sputtering and Atomic Layer Deposition, *Ceram. Int.*, 2019, **9**, p 11335–11341
28. Y. Ye, Y. Yao, H. Chen, S. Guo, J. Li and L. Wang, Structure, Mechanical and Tribological Properties in Seawater of Multilayer TiSiN/Ni Coatings Prepared by Cathodic Arc Method, *Appl. Surf. Sci.*, 2019, **493**, p 1177–1186
29. G. Li, L. Zhang, F. Cai, Y. Yang, Q. Wang and S. Zhang, Characterization and Corrosion Behaviors of TiN/TiAlN Multilayer Coatings by Ion Source Enhanced Hybrid Arc Ion Plating, *Surf. Coat. Technol.*, 2019, **366**, p 355–365
30. Y. Kim, T. Byun and J. Han, Superlattices and Microstructures Bilayer Period Dependence of CrN/CrAlN Nanoscale Multilayer Thin Films, *Superlattices Microstruct.*, 2009, **45**, p 73–79
31. B. Bouaouina, A. Besnard, S.E. Abaidia and F. Haid, Residual Stress, Mechanical and Microstructure Properties of Multilayer Mo2N/CrN Coating Produced by R.F Magnetron Discharge, *Appl. Surf. Sci.*, 2017, **395**, p 117–121
32. L. Ipaz, J. Caicedo, J. Esteve, F. Espinoza-beltran and G. Zambrano, Improvement of Mechanical and Tribological Properties in Steel Surfaces by Using Titanium- Aluminum/Titanium-Aluminum Nitride Multilayered System, *Appl. Surf. Sci.*, 2012, **258**, p 3805–3814
33. C. Dang, J. Li, Y. Wang and J. Chen, Structure, Mechanical and Tribological Properties of Self-toughening TiSiN/Ag Multilayer Coatings on Ti_6Al_4V Prepared by Arc Ion Plating, *Appl. Surf. Sci.*, 2016, **386**, p 224–233
34. J. Stallard, S. Poulat and D. Teer, The Study of the Adhesion of a TiN Coating on Steel and Titanium Alloy Substrates Using a Multi-mode Scratch Tester, *Tribol. Int.*, 2006, **39**, p 159–166
35. J. Caicedo, C. Amaya, L. Yate, O. Nos, M.E. Gomez and P. Prieto, Hard Coating Performance Enhancement by Using [Ti/TiN]n, [Zr/ZrN]n and [TiN/ZrN]n Multilayer System, *Mater. Sci. Eng. B*, 2010, **171**, p 56–61
36. X. Guan, Y. Wang, G. Zhang, X. Jiang, L. Wang and Q. Xue, Microstructures and Properties of Zr/CrN Multilayer Coatings Fabricated by Multi-Arc Ion Plating, *Tribol. Int.*, 2017, **106**, p 78–87
37. C. Tian, B. Yang, S. Yan, Z. Lu, Z. Huang and D. Fu, Influence of Substrate Rotation Speed on the Structure and Mechanical Properties of AlTiN/CrN Coatings, *Surf. Coat. Technol.*, 2013, **228**, p 228–232
38. C. Tavares, C. Vidrago, L. Rebouta, J.P. Rivie, E. Le Bourhis and M.F. Denanot, Optimization and Thermal Stability of TiAlN/Mo Multilayers, *Surf. Coat. Technol.*, 2005, **200**, p 288–292
39. S. Bull and A. Jones, Multilayer Coatings for Improved Performance, *Surf. Coat. Technol.*, 1996, **78**, p 173–184
40. Y. Wang and S. Zhang, Toward Hard Yet Tough Ceramic Coatings, *Surf. Coat. Technol.*, 2014, **258**, p 1–16
41. P. Yashar and W. Sproul, Nanometer Scale Multilayered Hard Coatings, *Vacuum*, 1999, **55**, p 179–190
42. S. Zhou, V. Pelenovich, B. Han, M. Yousaf, S. Yan, C. Tian and D. Fu, Effects of Modulation Period on Microstructure, Mechanical Properties of TiBN/TiN Nanomultilayered Films Deposited by Multi Arc Ion Plating, *Vacuum*, 2016, **126**, p 34–40
43. S. Barnett and M. Shinn, Plastic and Elastic Properties of Compositionally Modulated Thin Films, *Annu. Rev. Mater. Sci.*, 1994, **24**, p 481–511
44. S. Barnett and A. Madan, Superhard Superlattices, *Phys. World*, 1998, **11**, p 45–48
45. J. Yu, L. Dong, C. Li, Y. Pan, R. Wan, H. Gu and D. Li, The Influence of Modulation Periods on the Evolution of Microstructure and Mechanical Properties of Nanoscale HfN/HfB2 Multilayers, *Surf. Coat. Technol.*, 2017, **326**, p 368–374
46. S. Tien and J. Duh, Effect of Heat Treatment on Mechanical Properties and Microstructure of CrN/AlN Multilayer Coatings, *Thin Solid Films*, 2006, **494**, p 173–178
47. J. Caicedo, G. Bejarano, M. Gomez, P. Prieto and C. Cortéz, Nanostructured Multilayers of TiN/ZrN Obtained by Magnetron Sputtering, *Phys. Stat. Sol.*, 2007, **11**, p 4127–4133
48. Q. Zhang, Y. Xu, T. Zhang, Z. Wu and Q. Wang, Tribological Properties, Oxidation Resistance and Turning Performance of AlTiN/AlCrSiN Multilayer Coatings by Arc Ion Plating, *Surf. Coat. Technol.*, 2018, **356**, p 1–10
49. S. Zhou, S. Yan, B. Han, B. Yang, B. Lin, Z. Zhang, Z. Ai, V. Pelenovich and D. Fu, Influence of Modulation Period and Modulation Ratio on Structure and Mechanical Properties of TiBN/CrN Coatings Deposited by Multi-Arc Ion Plating, *Appl. Surf. Sci.*, 2015, **351**, p 1116–1121
50. A. Leyland and A. Matthews, On the Significance of the H/E Ratio in Wear Control: a Nanocomposite Coating Approach to Optimised Tribological Behaviour, *Wear*, 2000, **246**, p 1–11
51. Y. Zhou, R. Asaki, W. Soe, R. Yamamoto, R. Chen and A. Iwabuchi, Hardness Anomaly, Plastic Deformation Work and Fretting Wear Properties of Polycrystalline TiN/CrN Multilayers, *Wear*, 1999, **236**, p 159–164
52. J. Xu, H. Ju and L. Yu, Microstructure, Oxidation Resistance, Mechanical and Tribological Properties of Mo-Al-N Films by Reactive Magnetron Sputtering, *Vacuum*, 2014, **103**, p 21–27
53. C. Liu, F. Su and J. Liang, Nanocrystalline Co-Ni Alloy Coating Produced with Supercritical Carbon Dioxide Assisted Electrodeposition with Excellent Wear and Corrosion Resistance, *Surf. Coat. Technol.*, 2016, **292**, p 37–43
54. S. Huang, S. Chen, Y. Kuo, C. Wang, J. Lee, Y. Chan, H. Chen, J. Duh and T. Hsieh, Mechanical and Tribological Properties Evaluation of Cathodic Arc Deposited CrN/ZrN Multilayer Coatings, *Surf. Coat. Technol.*, 2011, **206**, p 1744–1752
55. T. Banerjee and A.K. Chattopadhyay, Structural, Mechanical and Tribological Properties of Pulsed DC Magnetron Sputtered TiN-WSx/TiN Bilayer Coating, *Surf. Coat. Technol.*, 2015, **282**, p 24–35
56. N. Beliardouh, K. Bouzid, C. Nouveau, B. Tlili and M.J. Walock, Tribological and Electrochemical Performances of Cr/CrN and Cr/CrN/CrAlN Multilayer Coatings Deposited by RF Magnetron Sputtering, *Tribol. Int.*, 2015, **82**, p 443–452
57. Y. Kong, X. Tian, C. Gong and P. Chu, Enhancement of Toughness and Wear Resistance by CrN/CrCN Multilayered Coatings for Wood Processing, *Surf. Coat. Technol.*, 2018, **344**, p 204–213
58. D. Kumar, N. Kumar, S. Kalaiselvam, S. Dash and R. Jayavel, Wear Resistant Super- Hard Multilayer Transition Metal-Nitride Coatings, *Surfaces and Interfaces*, 2017, **7**, p 74–82
59. S. Zhang, D. Sun, Y. Fu and H. Du, Toughening of Hard Nanostructural Thin Films: a Critical Review, *Surf. Coat. Technol.*, 2005, **198**, p 2–8
60. M. Nordin, M. Larsson and S. Hogmark, Mechanical and Tribological Properties of Multilayered PVD TiN/CrN, *Wear*, 1999, **232**, p 221–225
61. Z. Zhang, O. Rapaud, N. Allain, D. Mercs, M. Baraket, C. Dong and C. Coddet, Microstructures and Tribological Properties of CrN/ZrN Nanoscale Multilayer Coatings, *Appl. Surf. Sci.*, 2009, **255**, p 4020–4026